J Mater Sci (2006) 41:4865–4870
DOI 10.1007/s10853-006-0002-2

Effects of microstructure on oxygen transport in perovskite-type oxides

Qinghua Yin · Zhaohui Yang · Y. S. Lin

Received: 8 April 2005 / Accepted: 23 September 2005 / Published online: 4 May 2006

Abstract $La_{0.1}Sr_{0.9}Co_{0.9}Fe_{0.1}O_{3-\delta}$ (LSCF) particulates with different microstructures were prepared and oxygen sorption kinetics on these particulates was studied by a gravimetric method. The surface reaction on the crystallite surface is the rate-limiting step for oxygen sorption in loosely packed LSCF powders. In this case the sorption kinetics can be described by a linear driving force model with crystalline size independent sorption and desorption surface reaction rate constants. Oxygen sorption and transport rates are affected by the intercrystalline (grain boundary) resistance for LSCF particulates prepared with a press-sintering step, and in these cases both crystalline and particulate sizes determine the oxygen sorption rates. Sorption rate constant increases when increases the oxygen partial pressure of the atmosphere surrounding the LSCF samples.

Introduction

Perovskite-type oxides $La_{1-x}Sr_xCo_{1-y}Fe_yO_{3-\delta}$ (LSCF) have received much attention as membrane materials for air separation and syngas production applications [1–3] since the original work by Teraoka et al. [4–6]. Most studies on this series of materials were focused on the properties of the materials related to their applications as membranes [7–11] including the determination of oxygen nonstoichiometry, structural stability, electronic and ionic conductivity, and most importantly, oxygen permeability through these membranes. For oxygen permeation through a well-sintered perovskite type ceramic membrane, transport of oxygen is generally characterized by three steps in series: high pressure side surface reaction, bulk diffusion of oxygen anions (balanced with the transport of electron in an opposite direction), and lower pressure side surface reaction. The surface reaction step may consist of several sub-steps such as oxygen adsorption and charge transfer [12]. The relative significance of each contribution depends on membrane material composition and thickness, temperature and oxygen partial pressure gradient [10, 13–16]. In studying oxygen permeation through this type of materials, a characteristic thickness L_c was defined as the ratio of tracer diffusion coefficient to surface exchange coefficient. Surface exchange or bulk diffusion is predominant when the thickness of the membrane is smaller or larger than this value [17].

Recent studies have shown that the perovskite-type oxides can be also used as sorbents and sorbents/catalysts for high temperature air separation [2, 18] or partial oxidation reaction of methane [19] operated in the cyclic mode. In these applications, the perovsktie-type oxides are used in the particulate form consisting of loosely bound perovskite type oxide aggregates (or crystallites). Different from oxygen permeation through membrane, this separation/reaction process is based on the transient transport of oxygen into and out of the bulk crystallites of the material. Zeng and Lin [20] studied kinetics of oxygen sorption into and desorption from the LSCF particles by a transient thermogravimetry analysis (TGA) method. They found that the characteristic length for oxygen ion diffusion in the

Q. Yin · Y. S. Lin (✉)
Department of Chemical and Materials Engineering, Arizona State University, Tempe, AZ 85287-6006, USA
e-mail: Jerry.Lin@ASU.edu

Z. Yang · Y. S. Lin
Department of Chemical and Materials Engineering, University of Cincinnati, Cincinnati, OH 45221-0171, USA

bulk of the particle is small (in the micron range) and the step of the surface reaction on the particle surface can be considered as rate-limiting. Mantzavinos et al. [21] and Sahibzada et al. [22] also used the transient TGA method to study the oxygen sorption kinetics on perovskite type ceramic powders.

The microstructure of the perovskite-type oxide in the particulate form is quite different from that in the membrane form. The membrane consists of perovskite-type oxide crystallites with well-sealed grain boundary but the particulate may contain aggregates and crystallites with a certain grain boundary gaps depending on the processing method and conditions. It is important to understand how the microstructure of the perovskite-type oxide particulates affects the oxygen sorption in this group of particulate materials. The effects of oxygen partial pressure and temperature on oxygen sorption rates in the perovskite type ceramics are also important to the applications of this group of materials in the particulate form in separation and reaction processes. The objectives of this communication are to report the effects of the microstructure of perovskite type oxide particulate and oxygen partial pressure on oxygen sorption kinetics in the perovskite type ceramic particulates.

Experimental procedure

Perovskite-type oxide $La_{0.1}Sr_{0.9}Co_{0.9}Fe_{0.1}O_{3-\delta}$ was prepared by liquid citrate method. The details were given elsewhere [18]. After liquid citrate preparation and drying, organic compounds were burned out by self-ignition at 430 °C. The black ash-like products were ground into fine powder in mortar before the preliminary sintering at 600 °C. Five samples of different crystalline and/or aggregate sizes were prepared from the same batch of preliminary product. 1/3 amount of them was sintered at 1250 °C for 25 h. After sintering, the obtained products were then ground into powder, half amount of this powder was kept and marked as Sample #1, while the other half marked as Sample #2 after ball-milled for 7 days. Sample #3 was obtained by sintering another 1/3 amount of preliminary product at 950 °C for 15 h and grinding the sintered products into powder. The remaining amount of preliminary product was pressed into disks (300 MPa), and sintered at 950 °C for 15 h. After sintering, the disk was broken into small pieces, which was Sample #5. Sample #4 was obtained by grinding the small piece of the disk into powder in the mortar. The crystalline structure of the samples was examined by X-ray diffraction (XRD) ($CuK\alpha_1$). The crystalline sizes of the three samples were calculated using Scherrer equation. The surface area of the samples were measured by nitrogen adsorption porosimeter (Micromeritics ASAP2000). The measurements did not provide reliable surface area data because the particles were fairly large and dense, giving surface area too small to be measured accurately (< 0.01 m^2/g). Therefore, scanning electron microscope (SEM) (Hitachi S-4000) was used to estimate the aggregate size of the samples.

Kinetic study was conducted on a Cahn electronic balance (1000) detailed elsewhere [20]. Around 200 mg of $La_{0.1}Sr_{0.9}Co_{0.9}Fe_{0.1}O_{3-\delta}$ sample was placed into the sample pan, the sample was then heated to a designed temperature under certain gas atmosphere at a specific gas flow rate. Once the equilibrium was achieved, a sudden change of P_{O_2} in the gas phase was introduced to the system by switching the gas flow with different. P_{O_2} Oxygen sorption process occurred when P_{O_2} was changed from low to high, while desorption occurred when P_{O_2} was switched from high to low. The weight change of the sample was recorded continuously throughout the sorption or desorption process. He, dry air and O_2(Wright Brothers), were used to provide different P_{O_2} in the gas phase of the sample zone. all oxygen or desorption uptake curves of the samples were measured at flow rate of 200 mL/min. Five samples with different aggregate and crystalline sizes were studied to investigate the effect of particle size on the sorption kinetics.

Results and discussion

The average particle sizes of different samples were estimated from SEM photographs shown in Fig. 1. The particle size of the Sample #4 is smaller than 20 μm while the size of the pellet (Sample #5) is about 2 mm. The particle sizes of these five samples are listed in Table 1. XRD was conducted to confirm the perovskite structure of the as-prepared samples. Figure 2 gives the XRD patterns of the two powder samples sintered at 950 °C (A) and 1250 °C (B) and the membrane disk sample (C) sintered at 950 °C. The three samples exhibit typical perovskite structure. The calculated crystalline sizes of the samples are also given in Table 1. As seen from the calculation results, higher sintering temperature and longer sintering time give a larger crystalline size for the powder samples (Samples #1 and #2). Under the same sintering condition, the membrane samples (Samples #4, #5) have a smaller crystalline size, due to the less freedom for the growth of crystallites in the membrane disk.

Figure 3 shows a comparison of oxygen sorption (desorption) uptake curves between He–air and He-pure oxygen switches at 500 °C for Sample #3. W(e,a) and W(e,d) respectively refer to the equilibrium weight of sample in adsorption and desorption gas environment. The

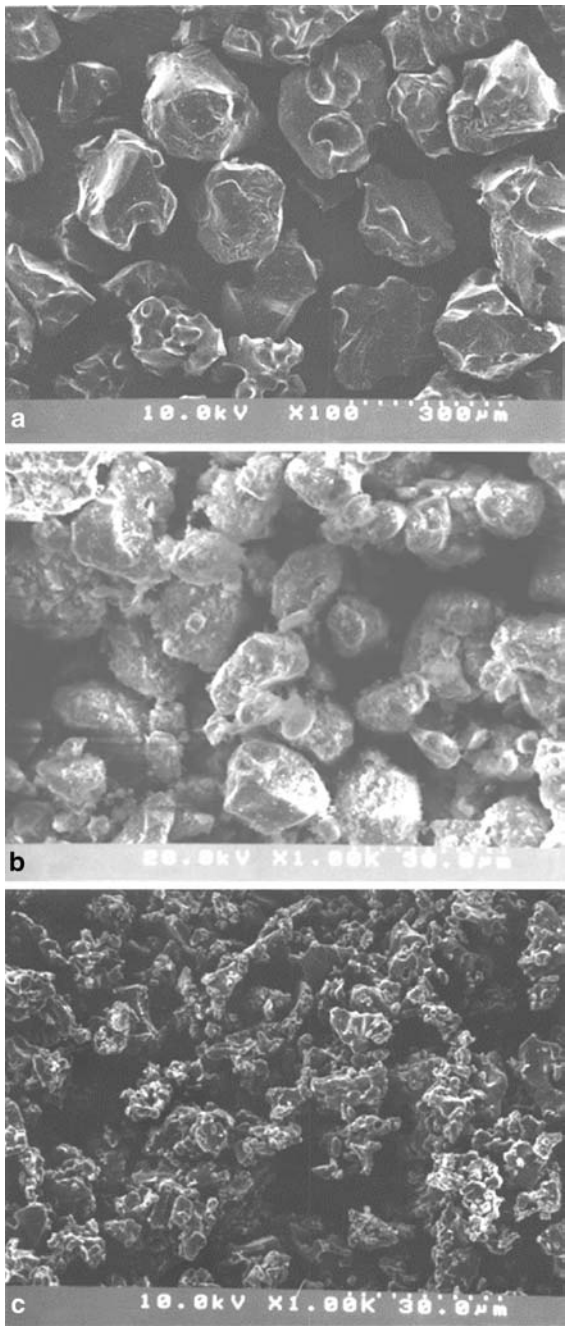

Fig. 1 SEM photographs of $La_{0.1}Sr_{0.9}Co_{0.9}Fe_{0.1}O_{3-\delta}$ samples. (**a**: Sample #1; **b**: Sample #2; **c**: Sample #3)

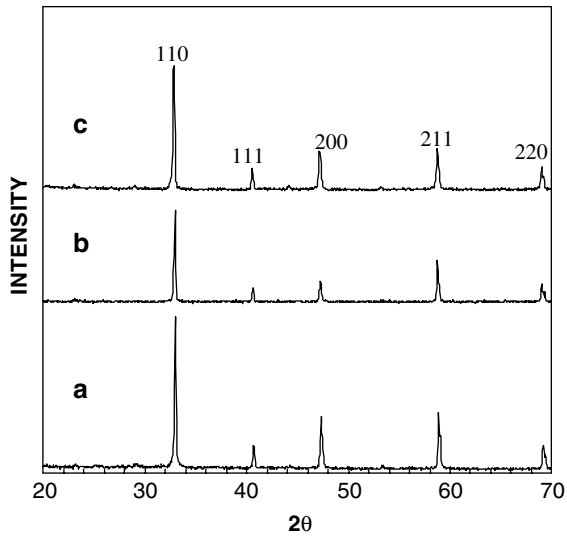

Fig. 2 XRD patterns of $La_{0.1}Sr_{0.9}Co_{0.9}Fe_{0.1}O_{3-\delta}$ samples. (**a**: Sample #3; **b**: Sample #1; **c**: Sample #5)

sample typically gained or lost respectively about 2–3% weight at equilibrium after He–air or air–He switch. The weight changes are normalized in Fig. 3 to show the kinetic effects. For oxygen sorption process between He and air, a fast weight gain was observed from the TGA curve in the adsorption period, in the desorption period, a much slower process was observed. A faster process was also observed in pure oxygen (higher oxygen partial pressure) than in air when in both cases the gas flow was switched from helium.

The difference in kinetics between sorption and desorption processes results from their different surface reaction rate constants. As described above, the average particle size of sample #3 is not larger than 10 μm. Normally, surface exchange is the rate-limited step in this particle size range. Van Hassel et al. [23] reported that the surface reaction rate in oxygen permeation through thin perovskite-type membrane in proportional to the difference of the oxygen vacancy between oxygen-rich and oxygen-lean sides. Therefore, a simple linear driving force model was proposed [20] to describe the oxygen transport into or out of the solid grains in the transient TGA experiment. For oxygen sorption and desorption periods,

Table 1 Sample information of $La_{0.1}Sr_{0.9}Co_{0.9}Fe_{0.1}\ O_{3-\delta}$

Sample #	Preparation method	Aggregate size (μm)	D_{hkl} (nm)	Adsorption at 500 °C	
				Initial slope (1/s)	95% decay time (s)
1	Sintered at 1250 °C for 25 h, and ground into powder	180	70.5	0.0206	54
2	Sample 1 ball-milled	20	70.5	0.0224	53
3	Sintered at 950 °C for 15 h, and ground into powder	≤10	61.6	0.0273	41
4	Pressed to disk, sintered, and ground to powder	≤20	47.8	0.0406	30
5	Pressed to disk, sintered, and crushed to pellets	~2 mm	47.8	0.0209	68

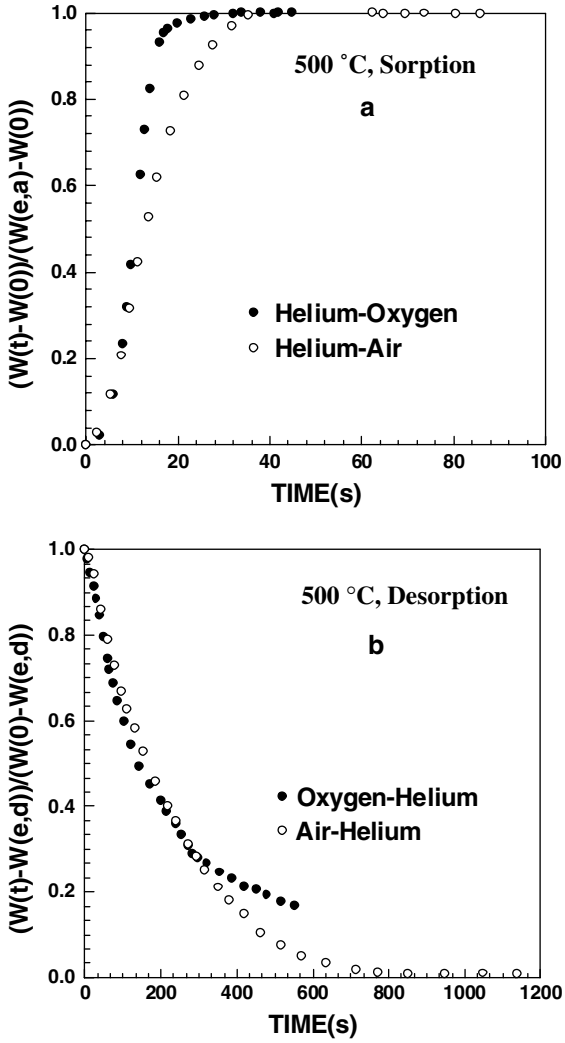

Fig. 3 Comparison of sorption (**a**) and desorption (**b**) kinetic curves between helium–air–helium and helium–oxygen–helium cycles

the model gave the following expressions to calculate the oxygen permeation flux:

$$J_{O_2} = k(C_v(e) - C_v(t)) \quad (1)$$

where k is the surface exchange rate constants respectively, $C_v(e)$ is the oxygen vacancy concentrations when the sample is in equilibrium in the P_{O_2} of sorption and desorption processes. In the He–air (sorption), air–He (desorption) switches, the initial driving forces, the deviation of oxygen vacancy concentration from the equilibrium, are identical. Thus, the difference in sorption and desorption curves reflects a difference in surface exchange reaction rate constant. The oxygen surface exchange rate for perovskite-type oxides increases with the equilibrium (final) oxygen partial pressure, $k = AP_{O_2}^n$ (with $n > 0$) [14–16, 22, 24]. He to O_2 switch gives larger driving force and rate constant, resulting in a faster sorption uptake as compared to He to air switch. Desorption curves are similar for the cases of air–He and O_2–He switches because k is same for both cases (as a result of same equilibrium oxygen partial pressure).

To investigate the effects of particle microstructure on the sorption process, oxygen sorption and desorption uptake curves were measured on the five samples of different aggregate or crystalline sizes summarized in Table 1. The initial slope and 95% decay time for the oxygen sorption uptake curves for the five samples are tabulated in Table 1. A smaller initial slope and larger decay time indicate a slower sorption rate. As shown in Table 1, Samples #1 and #2 have different aggregate size but same crystalline size, and they have similar sorption rates. This indicates that aggregate size does not affect the oxygen sorption/desorption rate in these cases. The faster sorption rate for Samples #3 as compared to Samples #1 and #2 is more likely due to its smaller crystalline size than its aggregate size. The effect of the crystalline size on sorption rate is more evident by comparison oxygen sorption rates on Samples #3 and #4. Sample #4 exhibits twice faster rates than Sample #3. The crystalline size of Sample #4 is much smaller than that of Sample #3. Obviously, the difference in the crystalline size can cause the significant difference in oxygen sorption rates between these two samples.

Samples #4 and #5 were made from the same membrane disk sintered at 950 °C. The difference is that Sample #4 was obtained by grinding the membrane disk into fine powder having average size of tens of microns, while Sample #5 by crushing the membrane disk into big pellets having the size of several millimeters. These two samples have same crystalline size. The sorption rate in Sample #4 is much faster than that on Sample #5. This suggests that for these two samples the particle (aggregate) size has a strong effect on oxygen sorption rate, different from the observations made for oxygen sorption on Samples #1, 2 and 3.

These results show that for loosely packed aggregates, crystalline size D_{hkl} determines the oxygen sorption rate, while the effect of aggregate size is negligible. This is because for aggregates formed by loosely packed crystals, the openings between these crystals (or grain boundary gaps) are large enough to eliminate possible resistance for oxygen transport from the bulk gas phase to the crystalline surface. For densely packed aggregates, such as Samples #4 and #5, the openings are significantly reduced as a result of pressing. In this case, oxygen transport resistance from gas phase to the crystalline surface is no longer negligible. Therefore both crystalline size and aggregate size play important roles in determining the oxygen sorption rate.

To quantitatively describe the effects of the crystalline size on the kinetics for aggregates formed by loosely packed crystals, we used the linear driving-drive force model (Eq. 1) to fit the experimental data to obtain the surface reaction rate constants. Assuming oxygen partial pressure independent k_a and k_d (a small step change of P_{O_2}), integrating a mass balance equation coupled with Eq. (1) gives the following equations that correlate the sample weight uptake to time [20]:
Sorption:

$$\frac{w(t)-w(0)}{w(e,a)-w(0)} = 1-\exp(-2\phi\ k_a t) \tag{2a}$$

Desorption:

$$\frac{w(t)-w(e,d)}{w(0)-w(e,d)} = \exp(-2\phi\ k_d t) \tag{2b}$$

where ϕ is the ratio of the surface area to volume of the perovskite type ceramic crystallites.

For comparison with the model, oxygen sorption uptake data were measured on Samples #1 and #4 between 0.00013 atm and 0.004 atm. The experimental data are shown in Fig. 4. As can be seen, the model fits the experimental data quite well. The regression results for the rate constants are given in Table 2. For the two samples with different crystalline sizes, the surface reaction rate constants are almost the same at the same temperature. These results further support that for loosely packed aggregates, it is the crystalline size that determines the oxygen sorption rate.

Conclusions

Gravimetric method can be used to study oxygen sorption kinetics and mechanisms for perovskite type ceramics. For loosely packed perovskite type ceramic particulates prepared without a pressing step, the rate-limiting step for oxygen sorption is the surface reaction on the perovskite type ceramic crystallite surface. In this case the crystalline size determines the oxygen transport rate. Intercrystalline (grain) boundary affects oxygen transport in perovskite type ceramic particulates and pellets prepared with a step of pressing. In these ceramic particulates or pellets both the crystalline and particulate size control oxygen sorption rates. Fast sorption and relatively slow desorption were observed in the experiment, which is partly due to the different surface reaction rates resulting from the different oxygen partial pressure in the gas phase in these two processes.

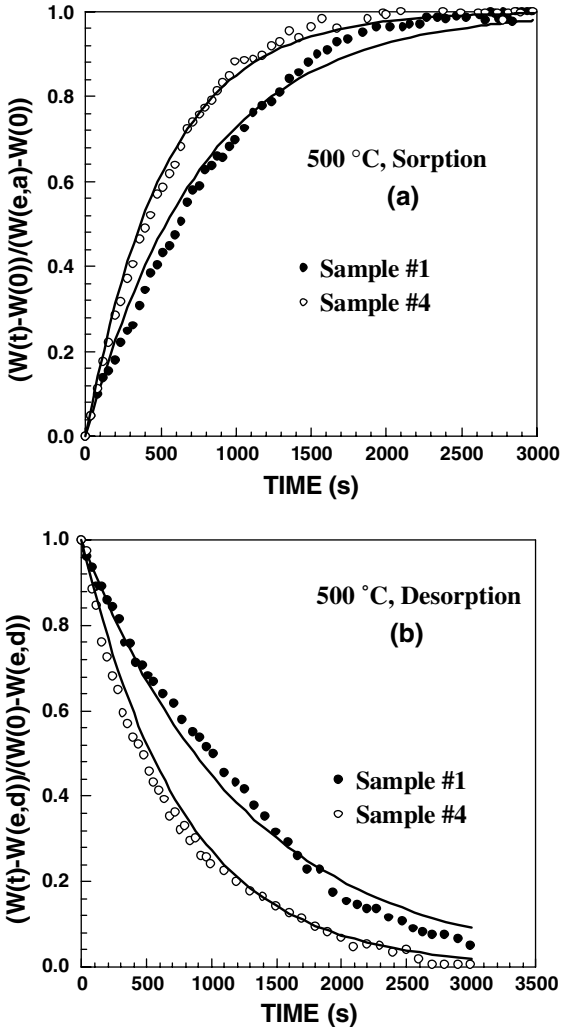

Fig. 4 Comparison of sorption (**a**) and desorption (**b**) kinetic curves between Samples #1 and #4 at 500 °C with P_{O_2} between 0.00013 atm and 0.004 atm

Table 2 Comparison of the model fitting results of sorption and desorption kinetics between Samples #1 and #4 at 500 °C with P_{O_2} changing between 0.00013 atm and 0.004 atm

Sample #	D_{hkl} (nm)	$\phi \cdot k_a$ (1/s)	$\phi \cdot k_d$ (1/s)	k_a (cm/s)	k_d (cm/s)
1	70.5	0.00065	0.0004	7.64×10^{-9}	4.70×10^{-9}
4	47.8	0.00095	0.0006	7.57×10^{-9}	4.78×10^{-9}

Acknowledgements The authors acknowledge the support of the NSF (CTS-0132694) on this project.

References

1. Dyer PN, Richards RE, Russek SL, Taylor DM (2000) Solid State Ionics 134(1-2):21
2. MacLean DL, Lin YS, Zeng Y (2000) US Patent 6,059,858

3. Lin YS, Kumakiri I, Nair BN, Alsyouri H (2002) Separ Purif Methods 32(2):229
4. Teraoka Y, Yoshimatsu M, Yamazoe N, Seiyama T (1984) Chem Lett 6:893
5. Teraoka Y, Zhang HM, Yamazoe N (1985) Chem Lett 9:1367
6. Teraoka Y, Zhang HM, Okamoto K, Yamazoe N (1988) Mater Res Bull 23(1):51
7. Mizusaki J, Yamauchi S, Fueki K, Ishikawa A (1984) Solid State Ionics 12(3):119
8. Mizusaki J, Yoshihiro M, Yamauchi S, Fueki K (1985) J Solid State Chem 58(2):257
9. Zhang HM, Shimizu Y, Teraoka Y, Miura N, Yamazoe N (1990) J Catal 121(2):432
10. Carter S, Selcuk A, Chater RJ, Kajda J, Kilner JA, Steele BCH (1992) Solid State Ionics 53(6):597
11. Liu LM, Lee TH, Qiu L, Yang YL, Jacobson AJ (1996) Mater Res Bull 31(1):29
12. Lin YS, Wang WJ, Han JH (1994) AICHE J 40(5):786
13. Ishigaki T, Yamauchi S, Kishio K, Mizusaki J, Fueki K (1988) J Solid State Chem 73(1):179
14. Kilner JA, DeSouza RA, Fullarton IC (1996) Solid State Ionics 86(8):703
15. Tenelshof JE, Lankhorst MHR, Bouwmeester HJM (1997) Solid State Ionics 99(1–2):15
16. Ten Elshof JE, Lankhorst MHR, Bouwmeester HJM (1997) J Electrochem Soc 144(3):1060
17. Bouwmeester HJM, Kruidhof H, Burggraaf AJ (1994) Solid State Ionics 72:185
18. Yang ZH, Lin YS, Zeng Y (2002) Ind Eng Chem Res 41(11):2775
19. Zeng Y, Tamhankar S, Ramprasad N, Fitch F, Acharya D, Wolf R (2003) Chem Eng Sci 58(3–6):577
20. Zeng Y, Lin YS (1998) Solid State Ionics 110(3–4):209
21. Mantzavinos D, Hartley A, Metcalfe IS, Sahibzada M (2000) Solid State Ionics 134(1–2):103
22. Sahibzada M, Morton W, Hartley A, Mantzavinos D, Metcalfe IS (2000) Solid State Ionics 136:991
23. Van Hassel BA, Kawada T, Sakai N, Yokokawa H, Dokiya M, Bouwmeester HJM (1993) Solid State Ionics 66(3–4):295
24. Steele BCH (2000) Solid State Ionics 134(1–2):3